Molecular dynamics simulation of nanofluidics and nanomachining

M. T. Horsch,[1, 4] S. Stephan,[1] S. Becker,[1] M. Heier,[1] M. P. Lautenschläger,[1]
F. Diewald,[2] R. Müller,[2] H. M. Urbassek,[3] and H. Hasse[1]

[1]Engineering Thermodynamics, [2]Applied Mechanics, [3]Computational Materials Science, University of Kaiserslautern, Germany,
[4]Chemical Engineering, IIT Kanpur, India

Computational Molecular Engineering

HPC & Big Data in Molecular Engineering
HiPC 2016, Hyderabad, December 19, 2016

NEMD simulation of heat transfer

Dual-control-volume[1] non-equilibrium molecular dynamics simulation:

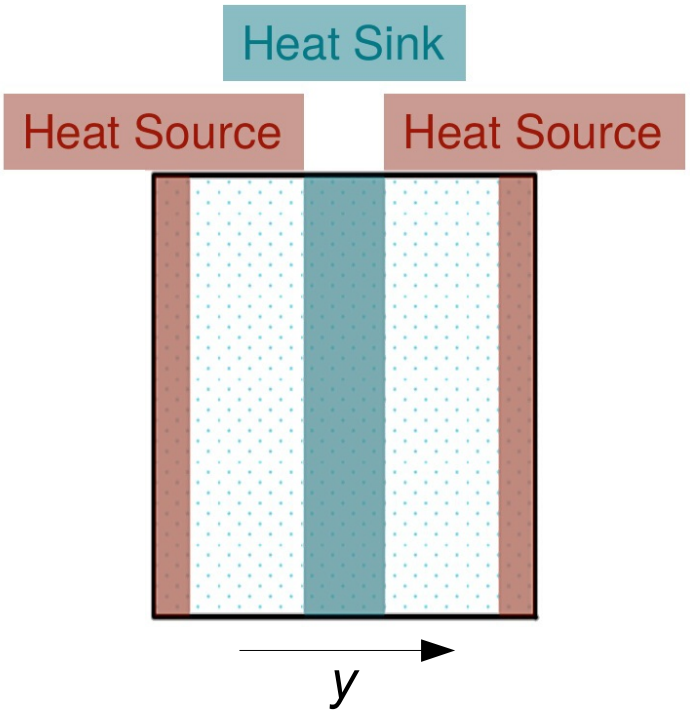

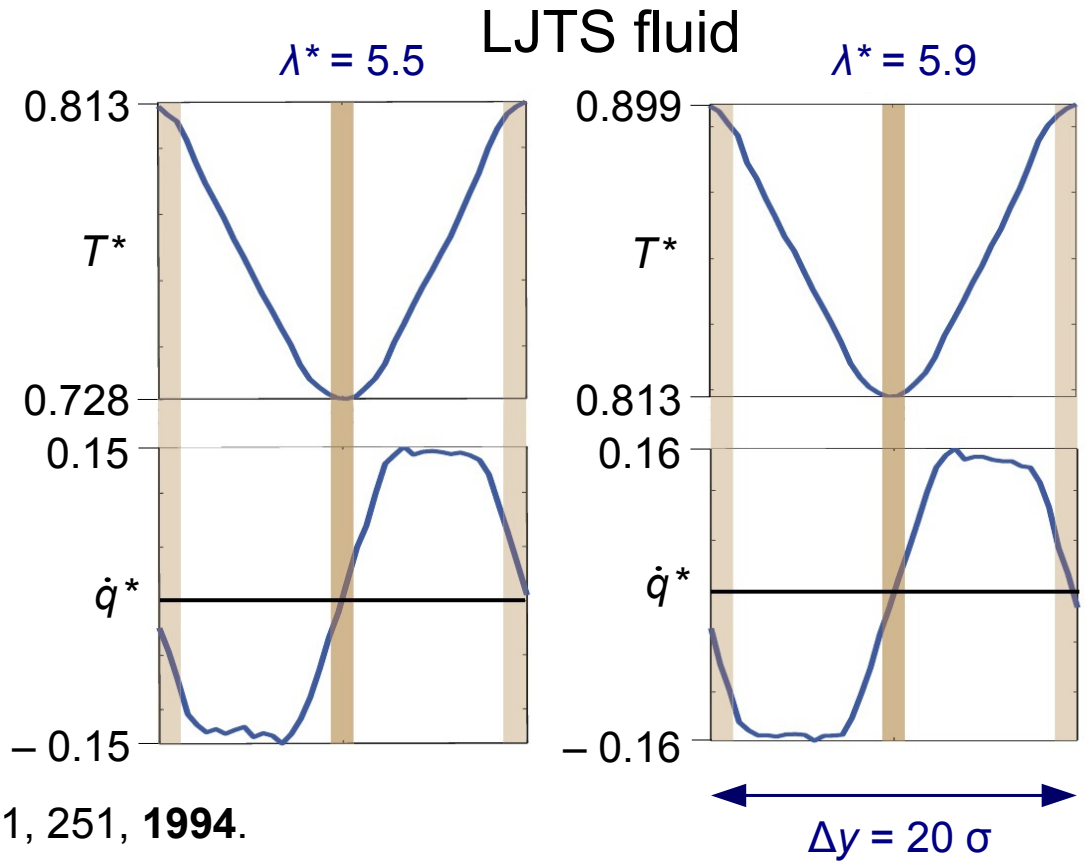

[1]T. Ikeshoji, B. Hafskjold, *Mol. Phys.* 81, 251, **1994**.

NEMD simulation of momentum transfer

By NEMD simulation, both linear and non-linear effects are accessible.

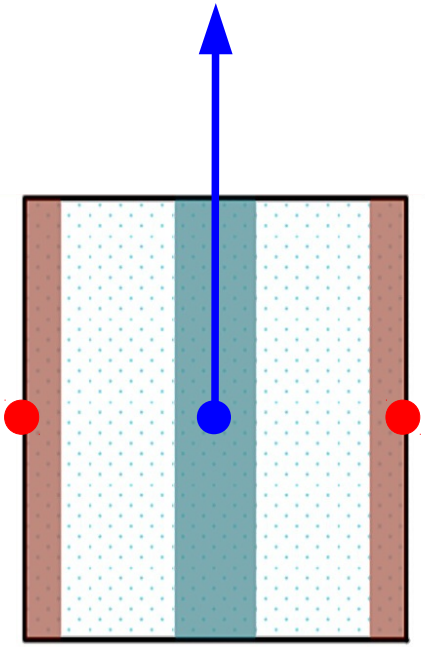

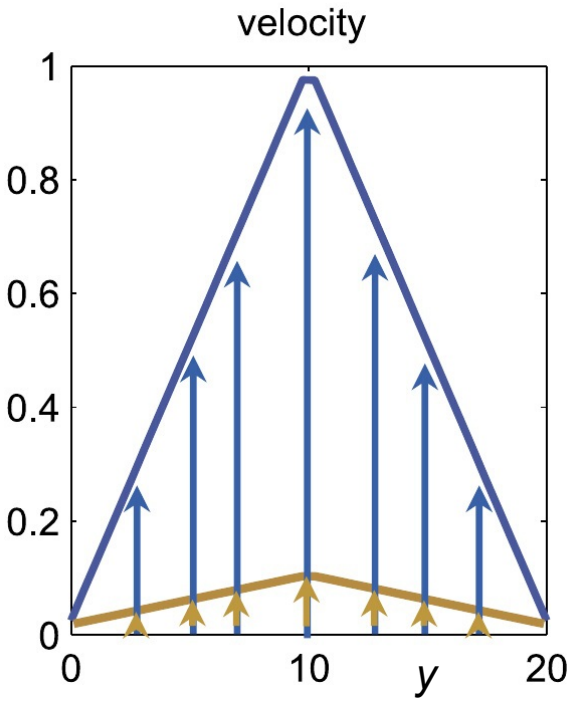

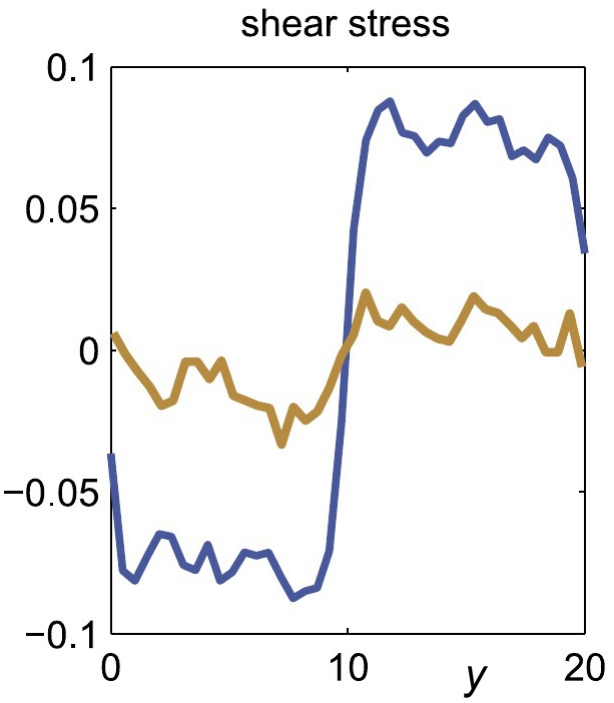

Hardy stress tensor: J. Vanegas, A. Torres, M. Arroyo, *J. Chem. Theory Comput.* 10, 691, **2014**.

NEMD simulation of momentum transfer

To compute the stress, kinetic and virial contributions are resolved locally.[1, 2]

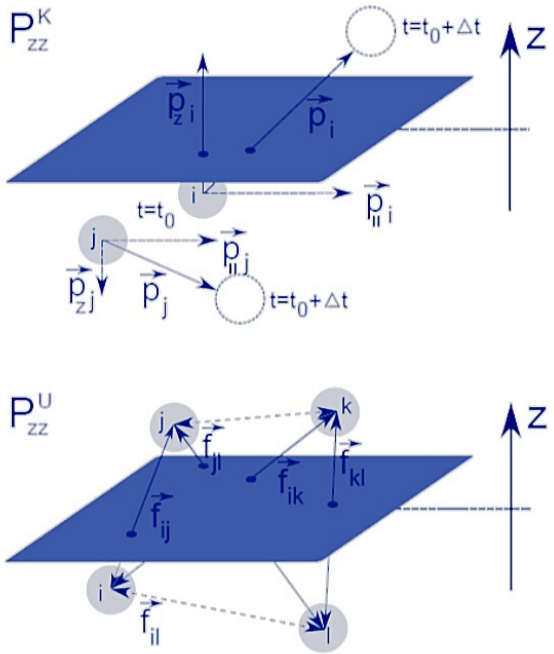

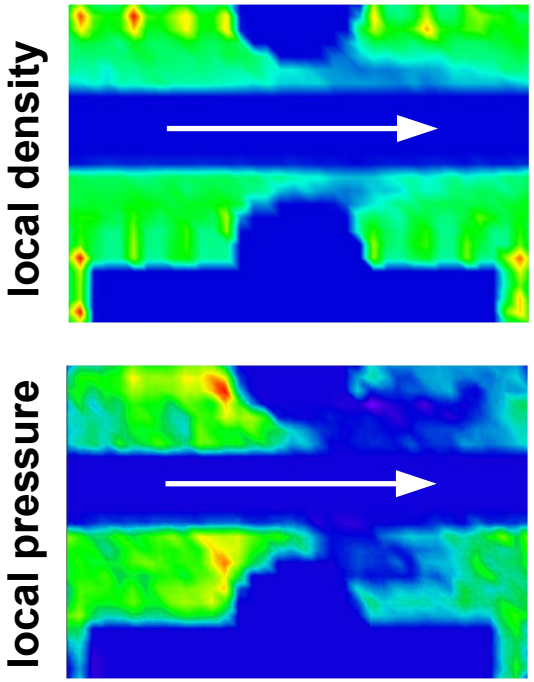

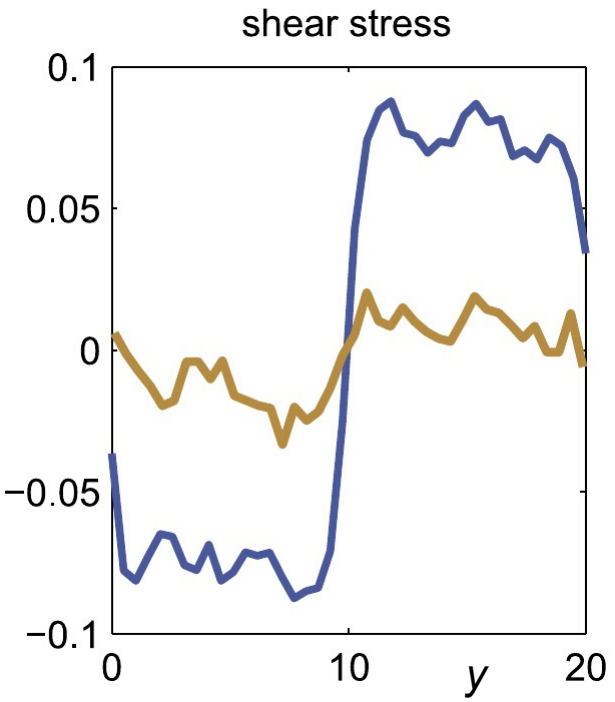

[1]Hardy stress tensor: J. Vanegas, A. Torres, M. Arroyo, *J. Chem. Theory Comput.* 10, 691, **2014**.
[2]MD simulation code *ls1 mardyn* available at **http://www.ls1-mardyn.de/**

NEMD simulation of diffusive mass transfer

Avendaño's dæmon,[1] based on **virtual colouring** of identical molecules, induces $\nabla\mu$ without the simultaneous presence of a pressure gradient by accelerating differently coloured molecules in opposite directions.

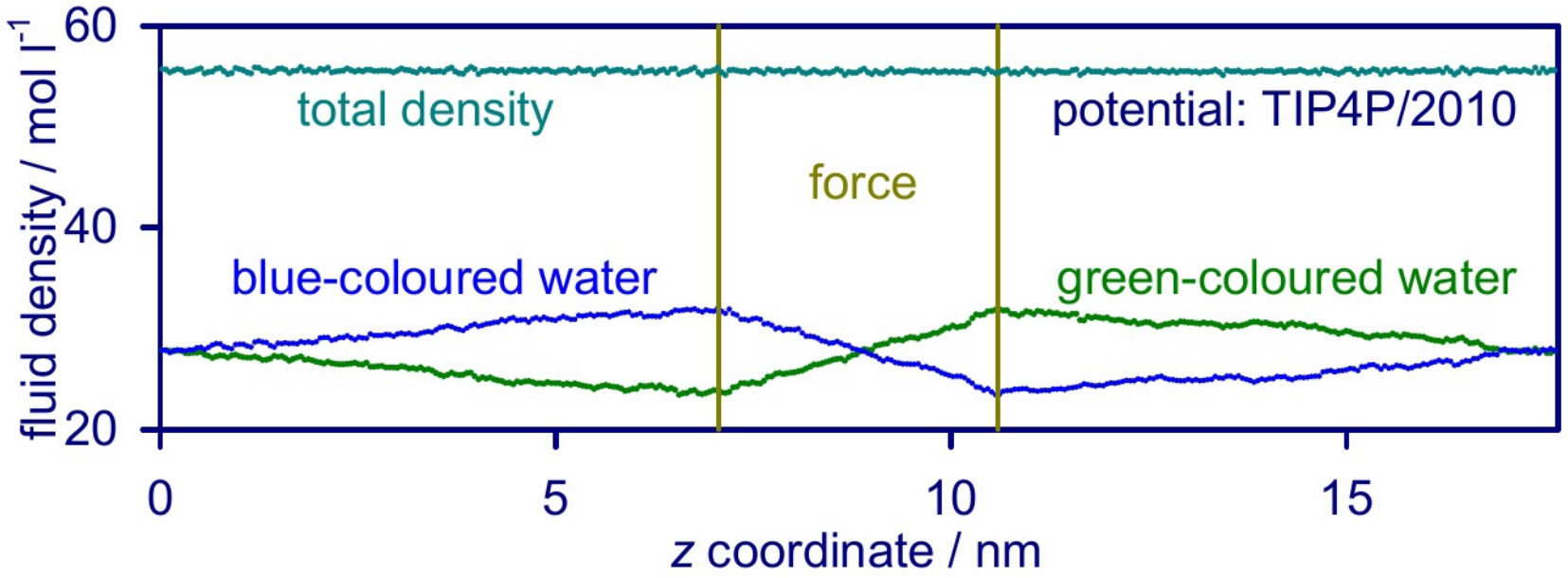

In this way, diffusive mass transfer is separated from momentum transfer.

[1]H. Frentrup, C. Avendaño, M. Horsch, A. Salih, E. A. Müller, *Mol. Sim.* 38, 540, **2012**.

NEMD simulation of Poiseuille flow

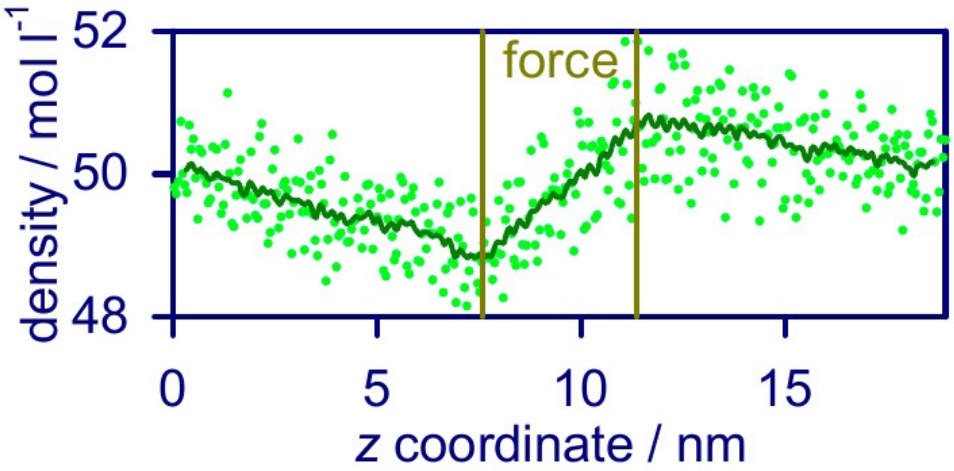

The accelerating force is only applied to the fluid molecules within a specified control volume.

It overcompensates the pressure drop, so that (equivalent) density, pressure, and chemical potential gradients are actually present.

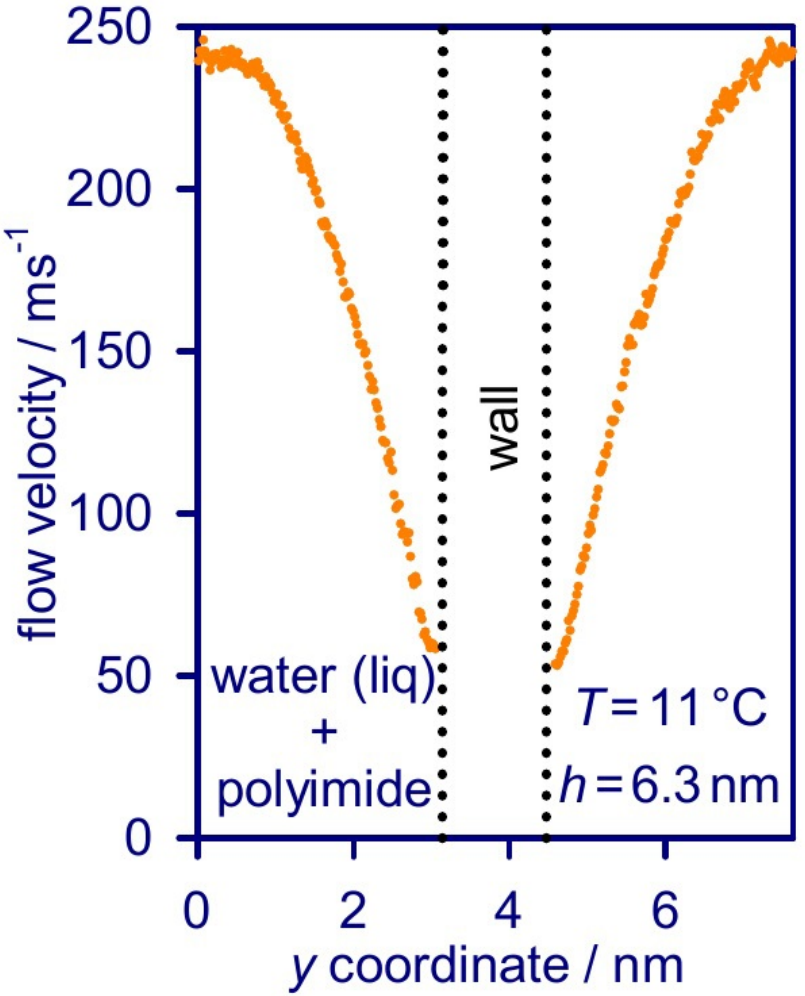

NEMD simulation of Poiseuille flow

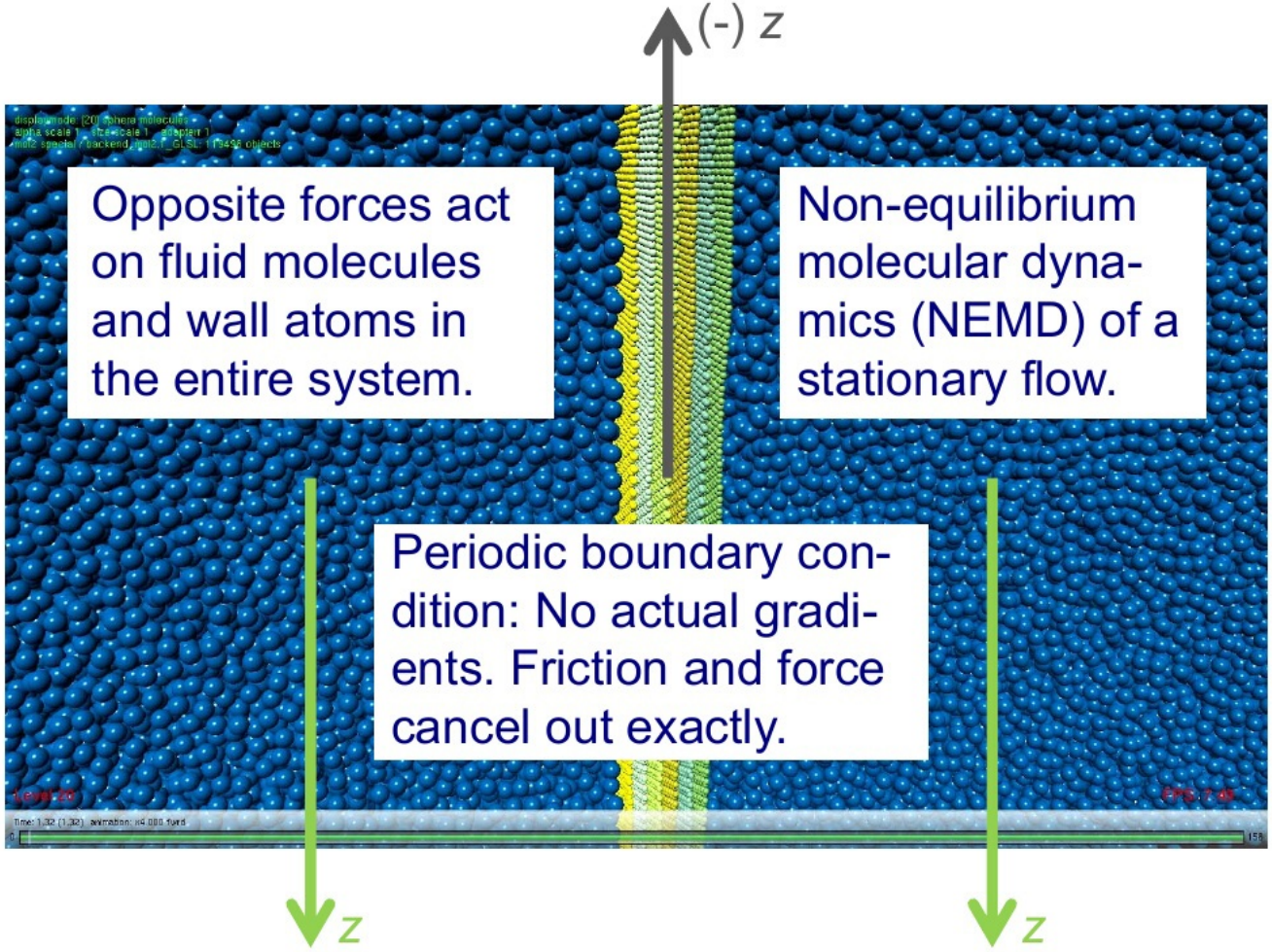

NEMD simulation of Poiseuille flow

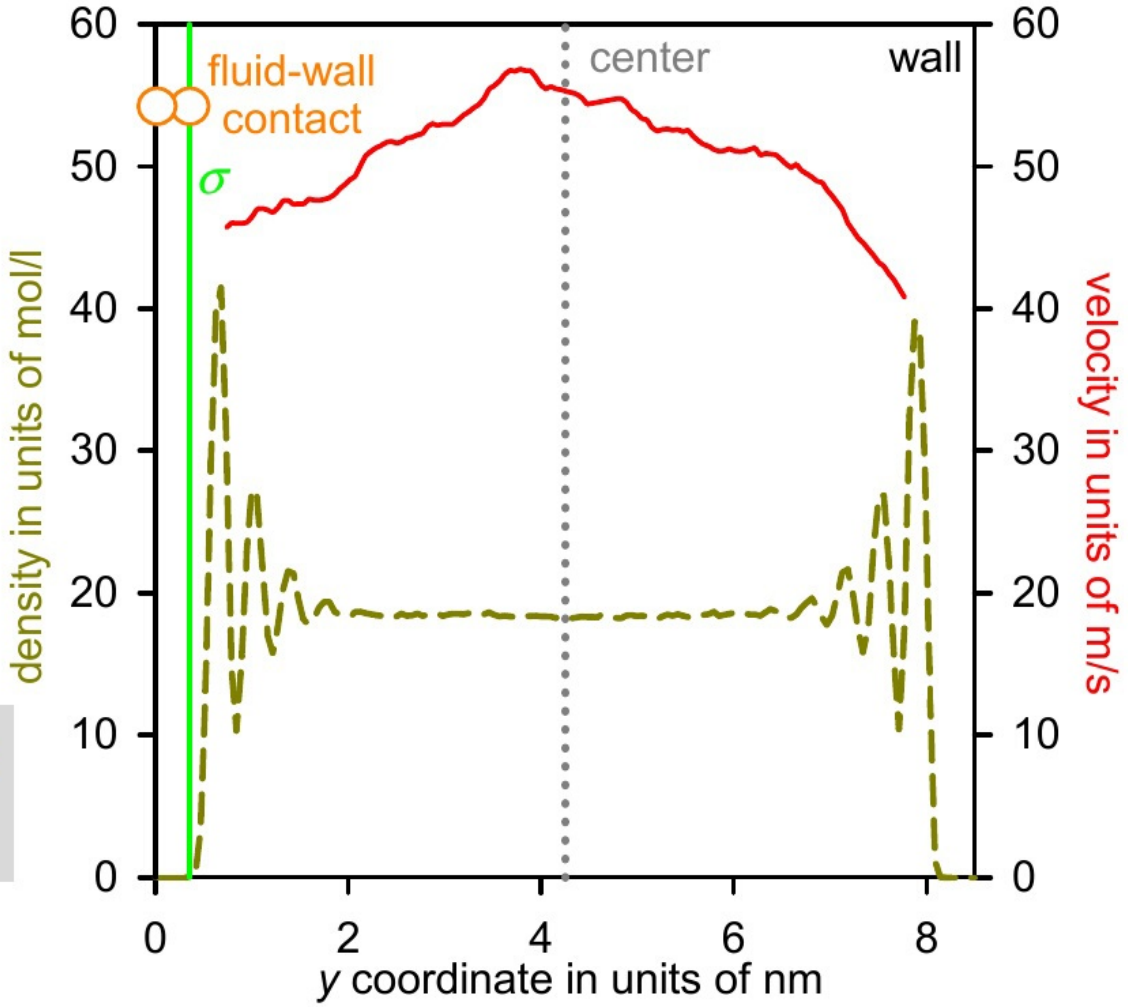

Methane in graphite

T = 166 K

Methane at a graphite wall: Presence of slip

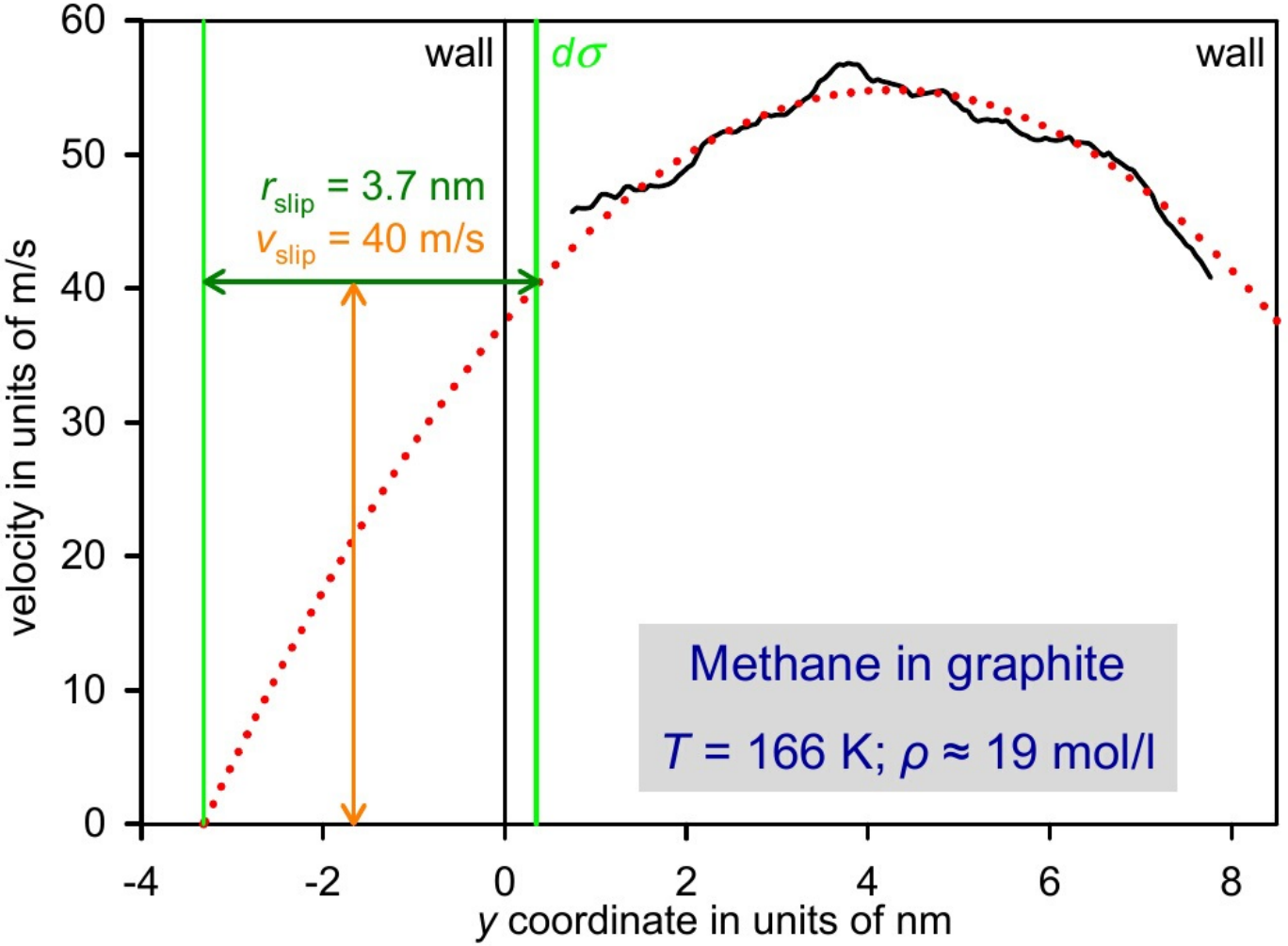

Water in a polar membrane: Absence of slip

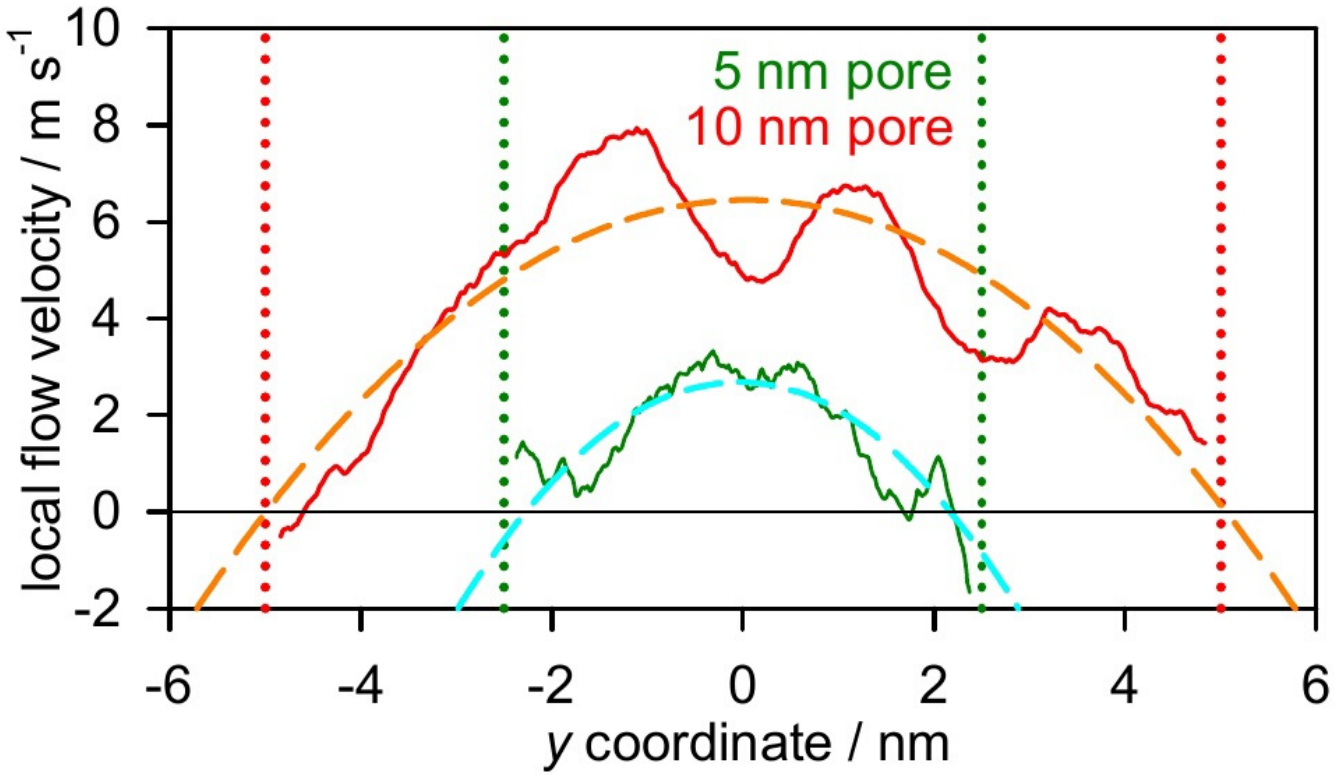

boundary slip practically negligible, in contrast to the unpolar system

r_{slip} approaches the nm length scale at high flow velocities (200 m/s)

Quantitative water model: TIP4P/2010 (Huang *et al.*)

Qualitative P84 polyimide pore model: Graphite with superimposed point charges

Contact angle and fluid-wall interaction

LJTS potential for fluid (f) and wall (w) with $\sigma_{fw} = \sigma_f$ und $\varepsilon_w = 100\ \varepsilon_f$.

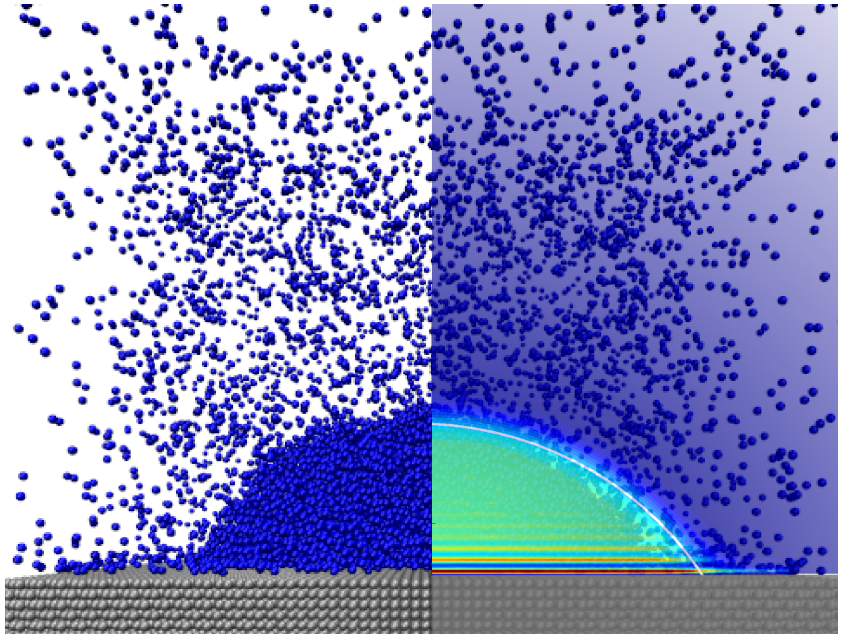

S. Becker *et al.*, *Langmuir* 30, 13606, **2014**

Correlation of the density profile by

$$\rho(r, y) = f(r) \cdot [h(y) + 1],$$

with the exponential decay term $h(y)$

and a hyperbolic tangent profile $f(r)$.

Variation of the temperature T and the fluid-wall dispersion by $\zeta = \varepsilon_{fs} / \varepsilon_f$.

Contact angle and fluid-wall interaction

Variation of the reduced fluid-wall dispersion energy ζ, at constant T:

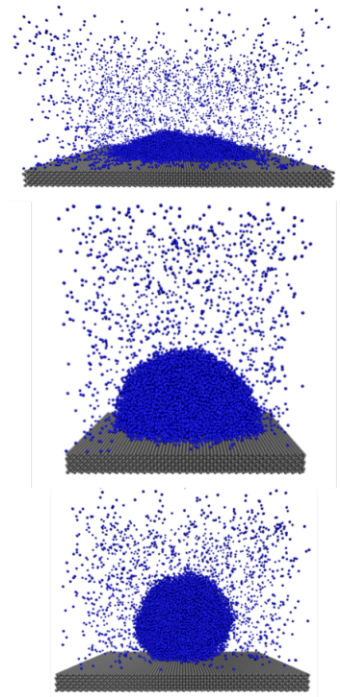

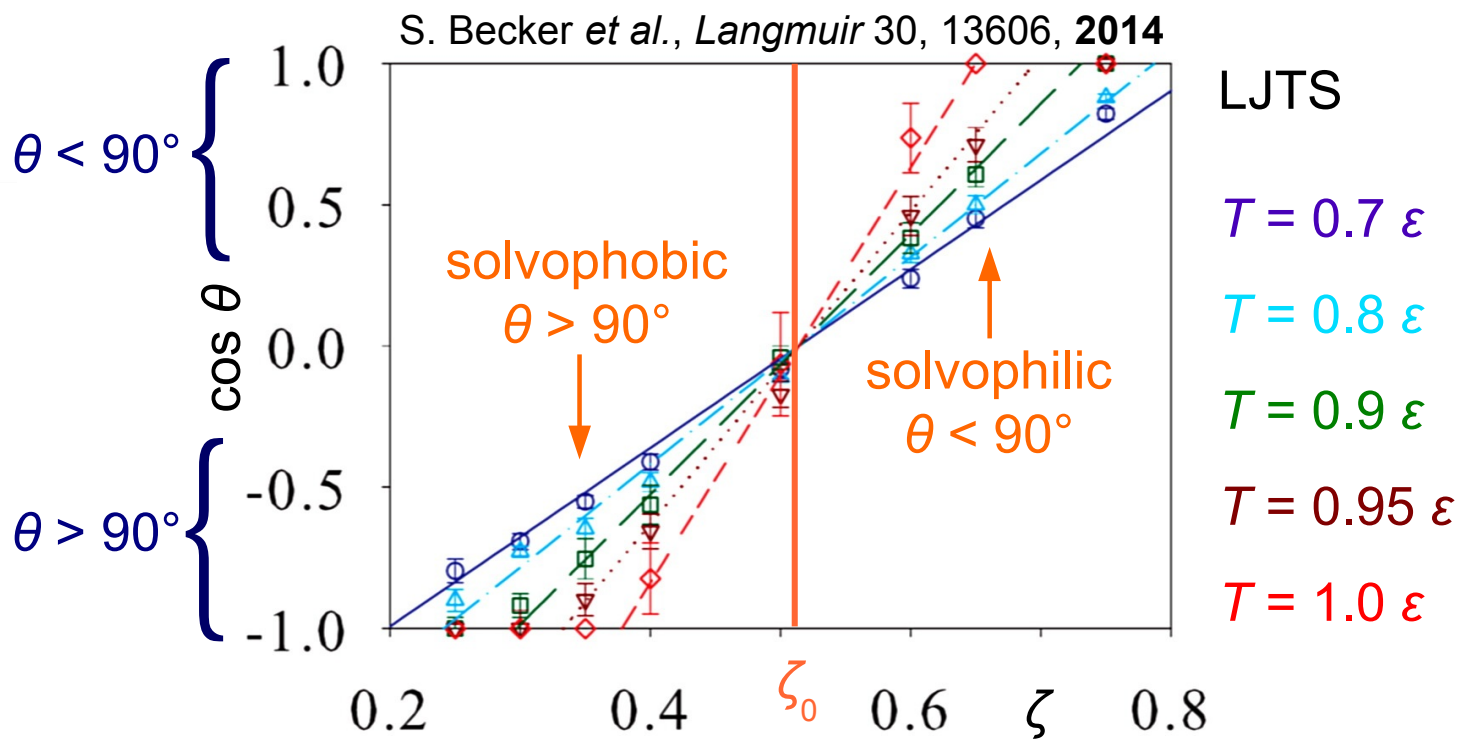

Correlation: cos θ proportional to $\zeta - \zeta_0$ for $\zeta_0 = 0.52$ at all temperatures.

Contact angle and fluid-wall interaction

At high temperatures, (pre-)critical wetting occurs:

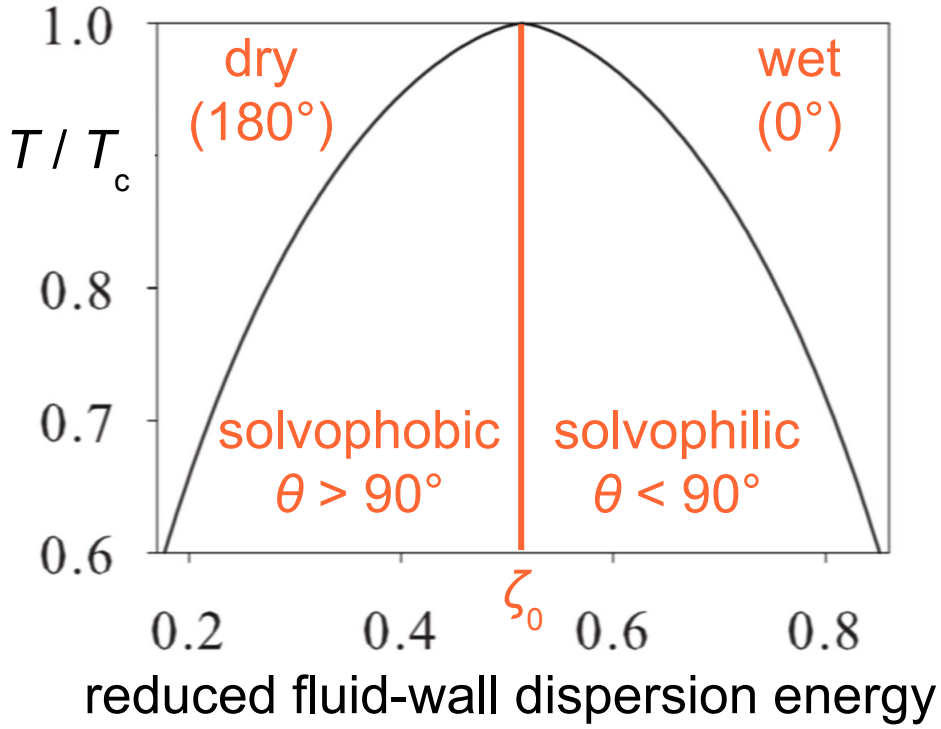

LJTS wall with
$\sigma_s = \sigma_f$ and
$\rho_s = 1.07\ \sigma_f^{-3}$

[1] S. Becker, H. M. Urbassek, M. Horsch, and H. Hasse, *Langmuir* 30, 13606, **2014**.

Correlation:[1] $\cos\theta$ proportional to $\zeta - \zeta_0$ and to $(1 - T/T_c)^{-2/3} + 1$.

NEMD simulation of Couette shear flow

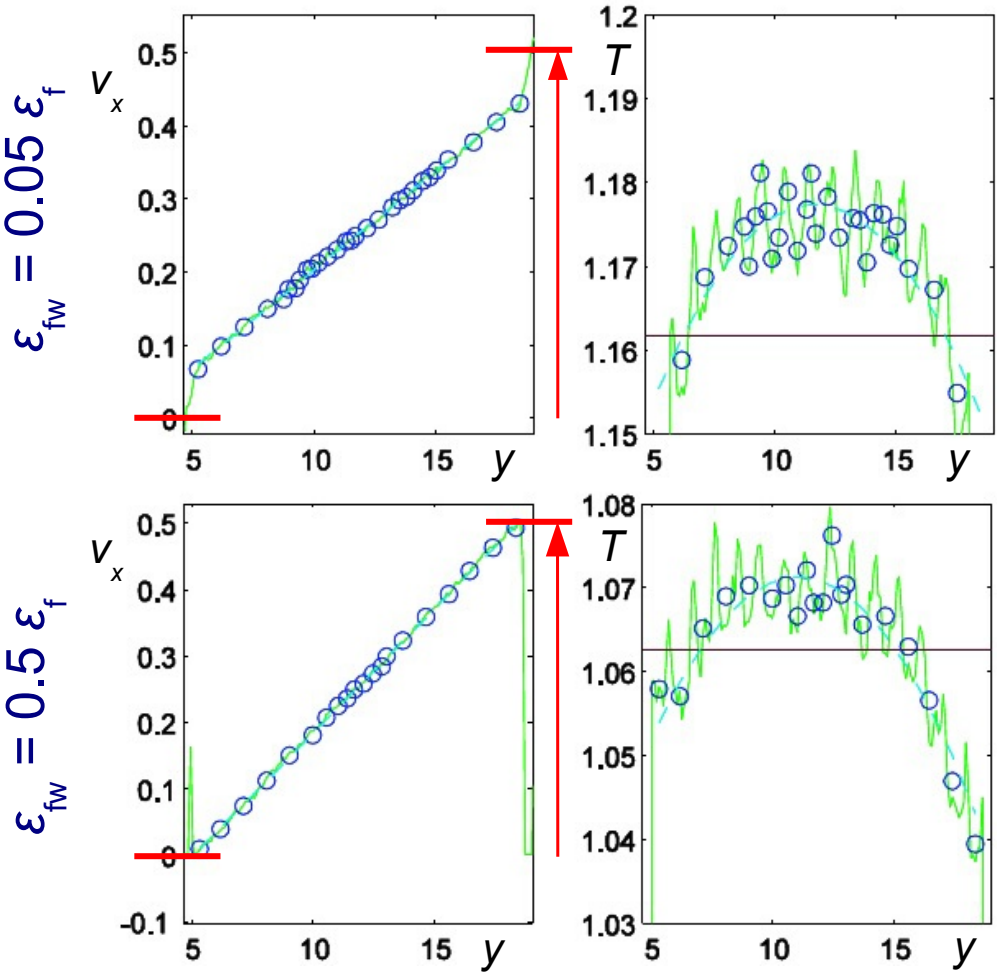

Scenario: Fluid and wall as LJTS with $\varepsilon_w = 100\ \varepsilon_f$ and $\sigma_w = \sigma_f$

$$T_w = 0.8\ \varepsilon_f$$
$$\Delta y_w = 15\ \sigma_f$$
$$\Delta v_w = 0.5\ (\varepsilon_f / m_f)^{1/2}$$

Fluid **attracted more strongly** to the walls supports greater shear rates **without boundary slip**. A stronger unlike interaction between the fluid and the wall **improves heat transfer** from the fluid to the wall.

Nanomachining with a rigid nanoindenter[1, 2]

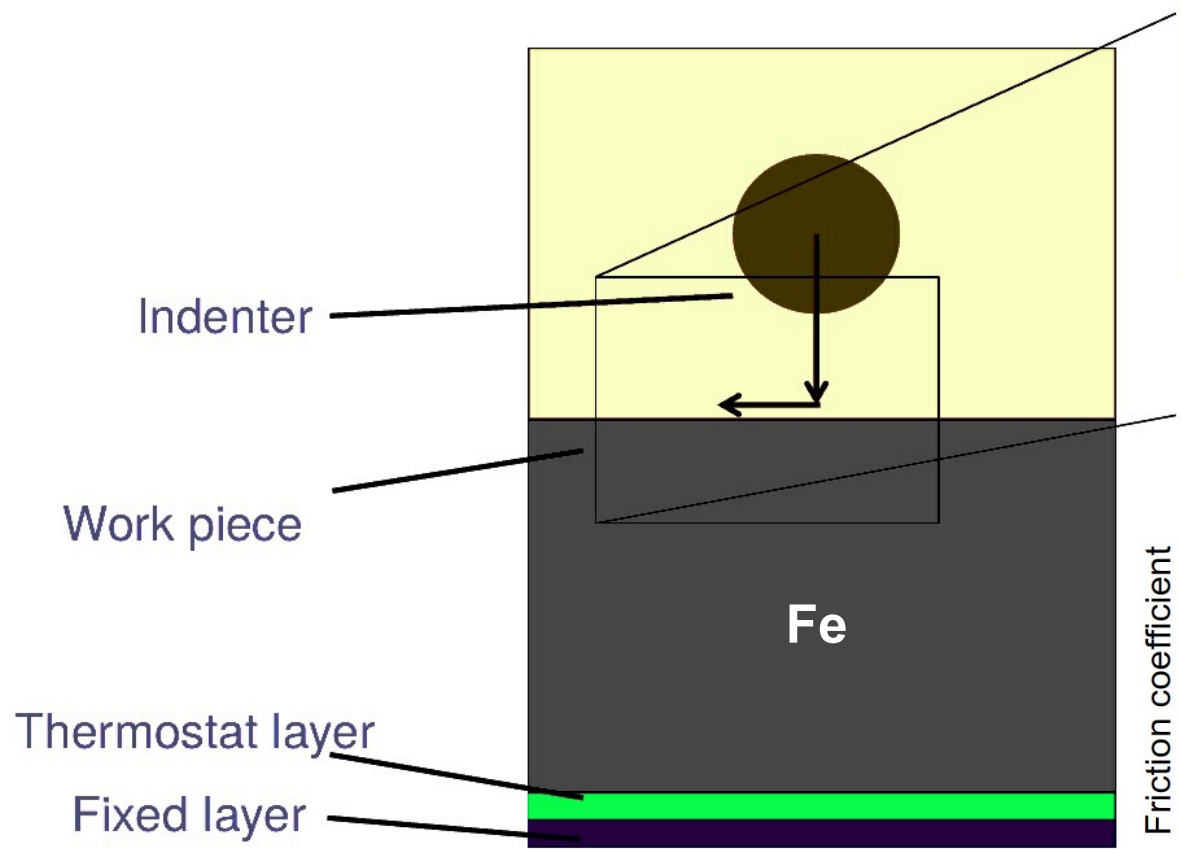

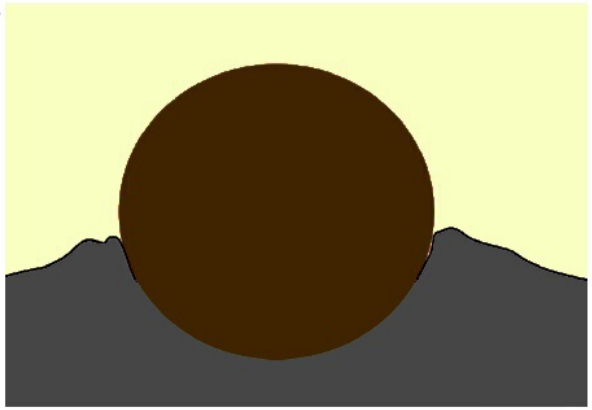

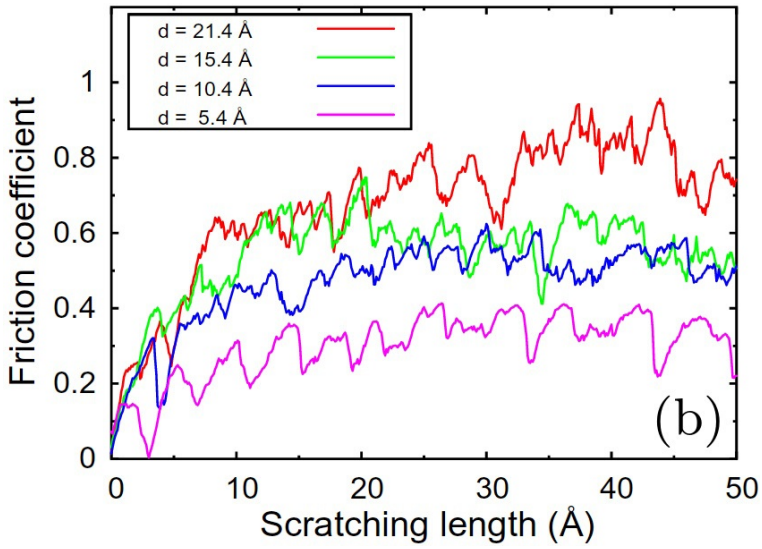

[1]Y. Gao *et al.*, *Comput. Mater. Sci.* 103, 77, **2015**.

[2]Y. Gao, H. M. Urbassek, *Appl. Surf. Sci.* 389, 688, **2016**.

Nanomachining in the presence of a liquid

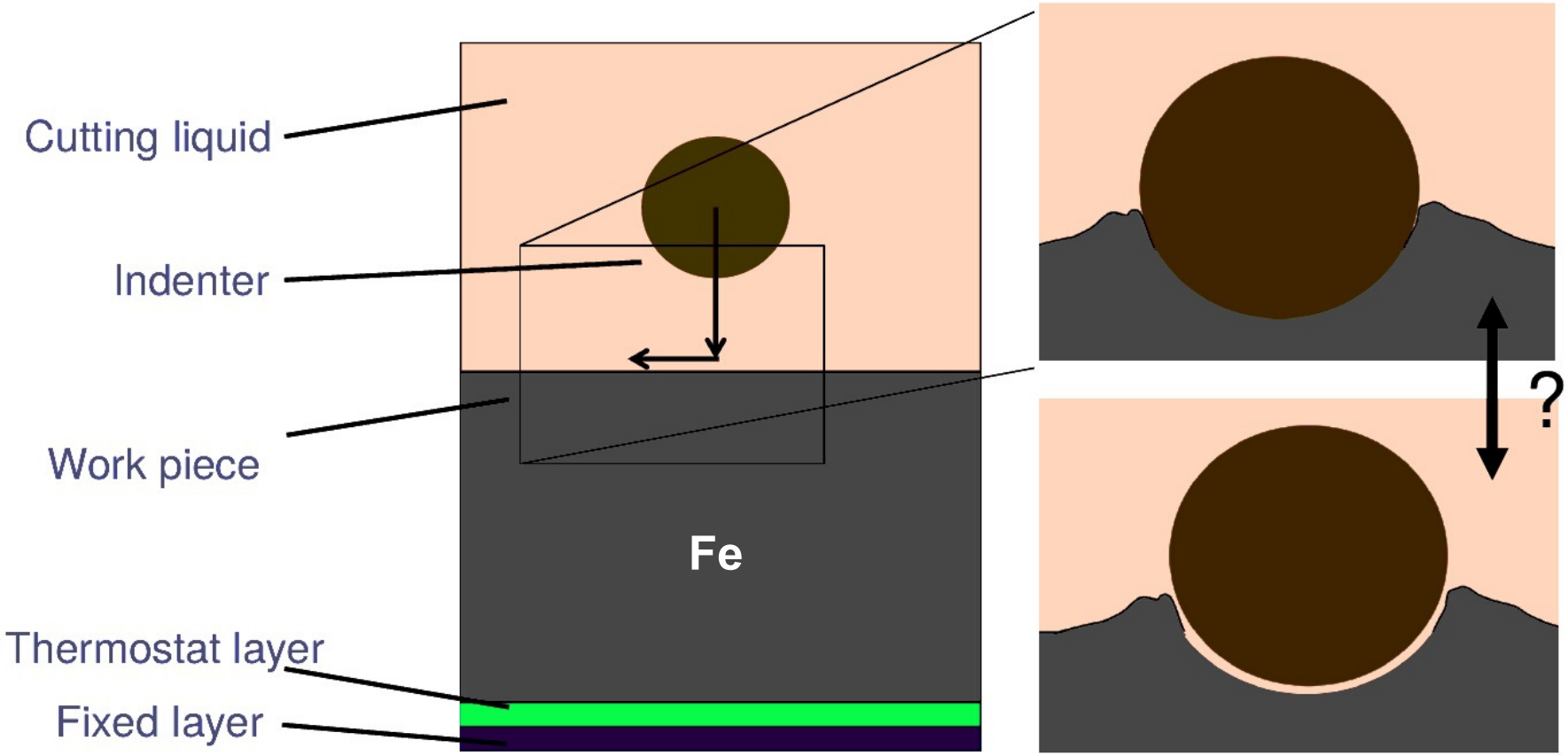

Nanomachining in the presence of a liquid

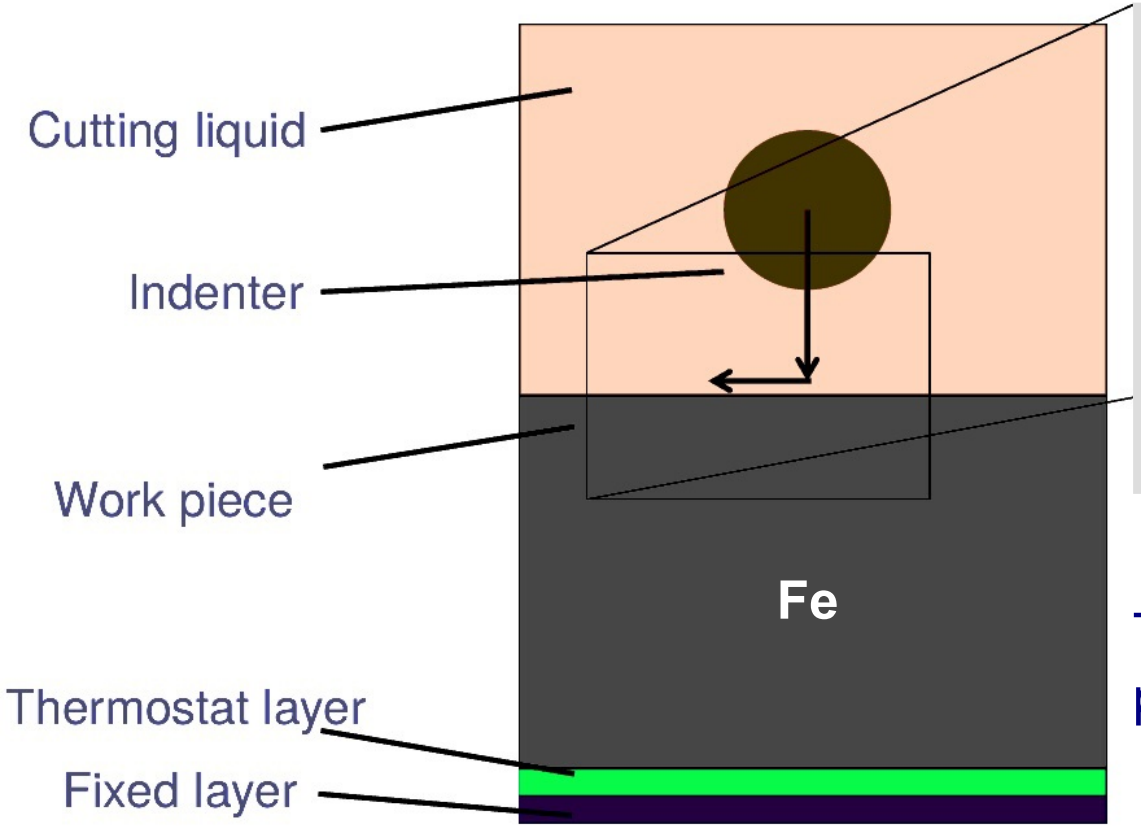

Fluid and fluid-solid: LJTS

Fluid-solid: $\zeta = 0.5$

Iron: Mendelev potential[1]

Indenter: Rigid cylinder (with LJTS sites)

Thermostat acting on remote part of the work piece,

$$T_{ext} = 0.8\,\varepsilon_f,$$

fluid density $\rho_f = 0.8\,\sigma^{-3}$.

[1]M. Mendelev, S. Han, D. Srolovitz, G. Ackland, D. Sun, M. Asta, *Philos. Mag.* 83, 3977, **2003**.

Indentation in the presence of a liquid

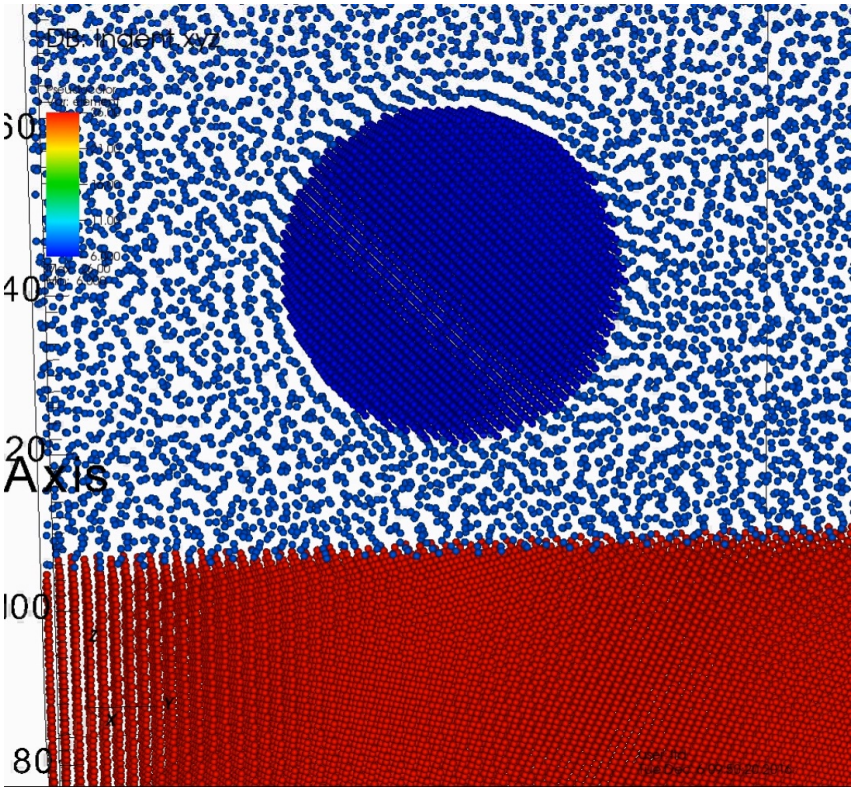

Fluid and fluid-solid: LJTS

Fluid-solid: $\zeta = 0.5$

Iron: Mendelev potential

Indenter: Rigid cylinder (with LJTS sites)

Thermostat acting on remote part of the work piece,

$$T_{ext} = 0.8\ \varepsilon_f,$$

fluid density $\rho_f = 0.8\ \sigma^{-3}$.

Scratching in the presence of a liquid

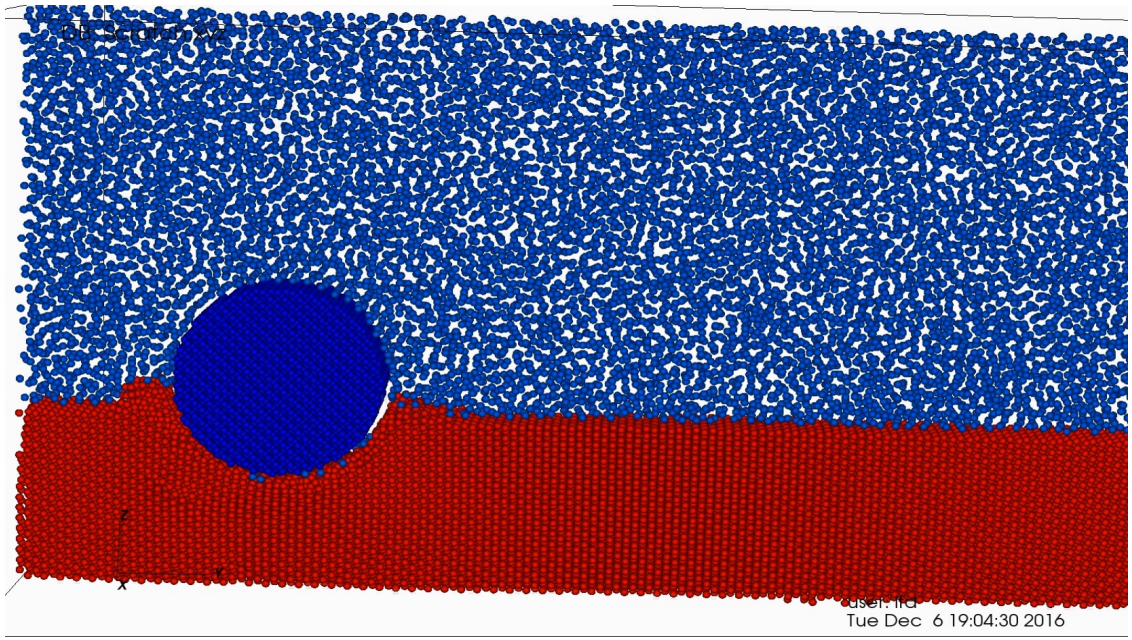

The LJTS fluid with $\zeta = 0.5$ does not lubricate the nanomachining process.

Heat transfer from work piece to liquid

MD simulation of indentation and scratching with different orders of magnitude for the fluid-solid interaction.

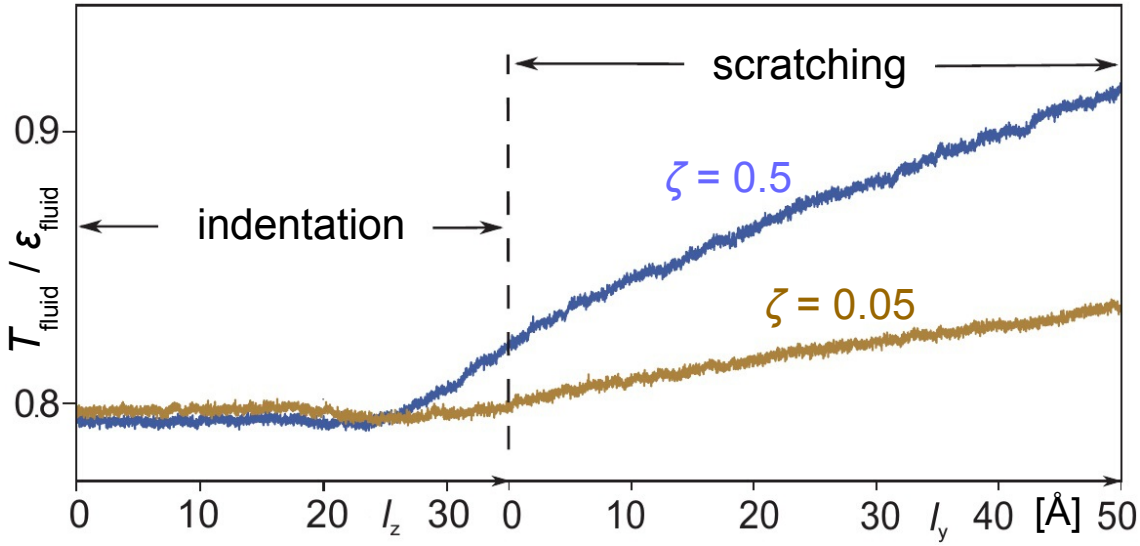

temperature profile (ζ = 0.5)

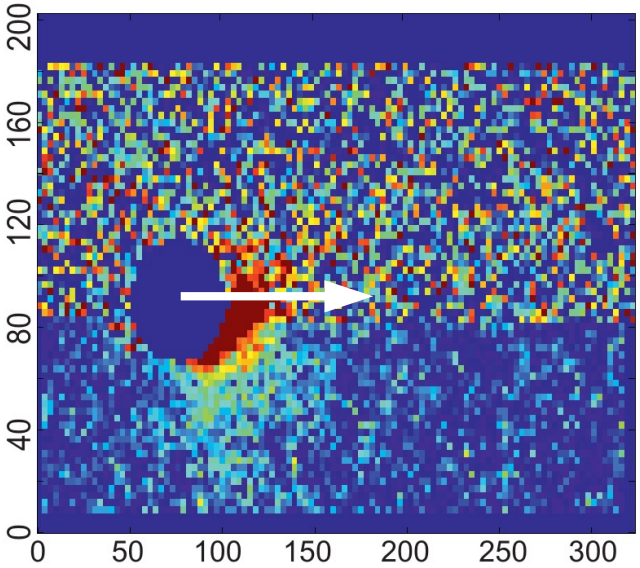

Heat transfer from work piece to liquid

MD simulation of indentation and scratching with different orders of magnitude for the fluid-solid interaction.

temperature profile ($\zeta = 0.5$)

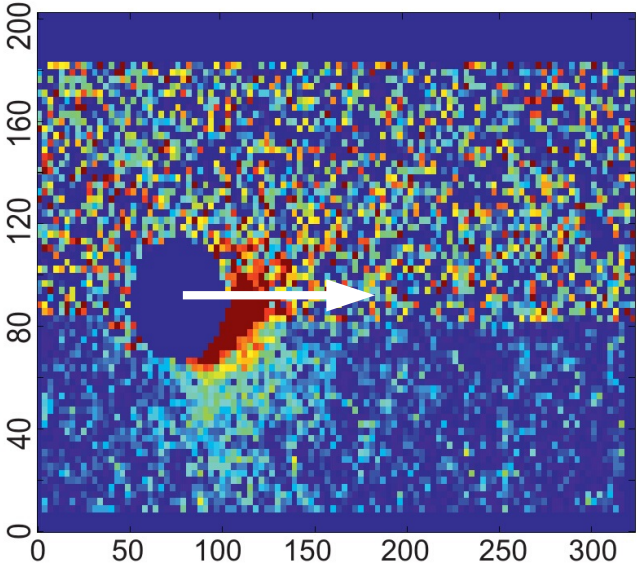

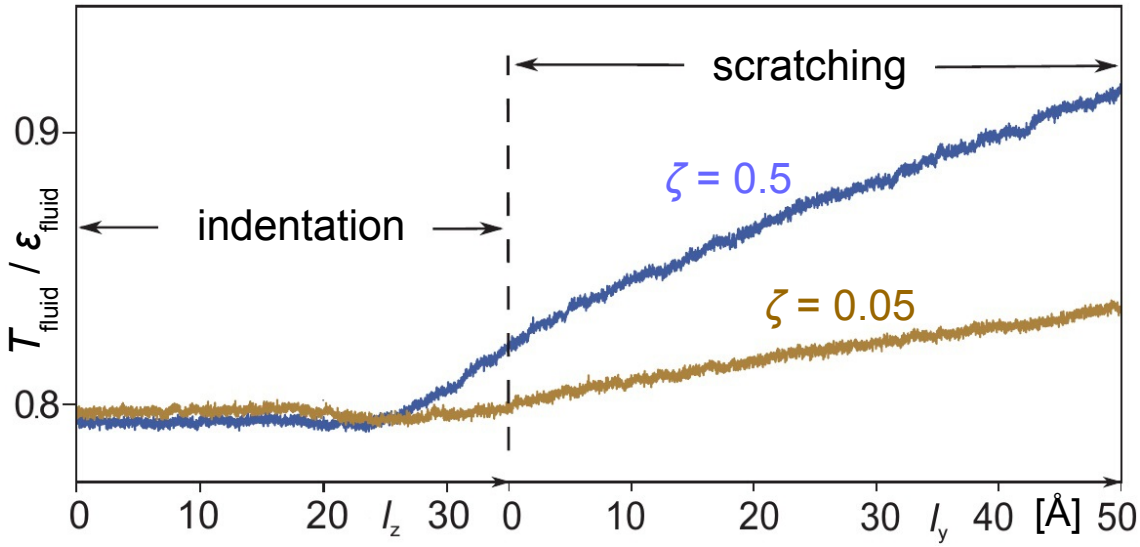

Greater fluid-wall dispersion

- reduces Kapitza (thermal) resistance
  here, by 10 to 50%, depending on T
- increases friction → no lubrication by LJ
  here, F_T/F_N increased by 20 to 30%

Morphology as a challenge for data science

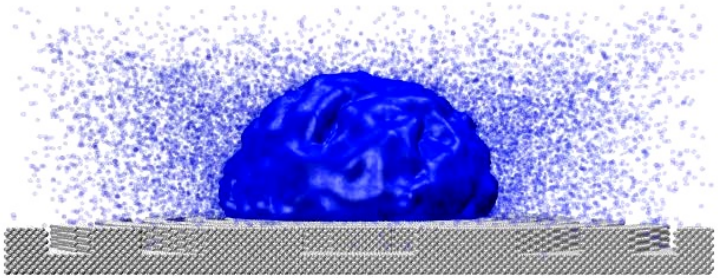

Physical and chemical inhomogeneities influence adsorption and wetting.

Nanoscopic Poiseuille flow: Results

Methane in graphite: T = 166 K; values of η and ξ from Wang *et al.*

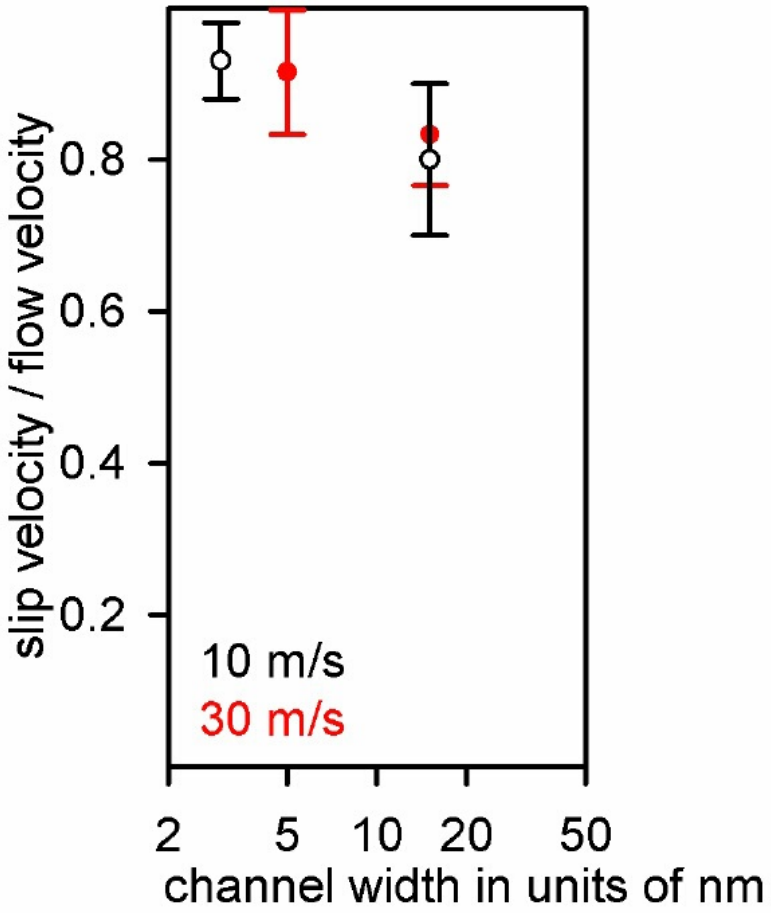

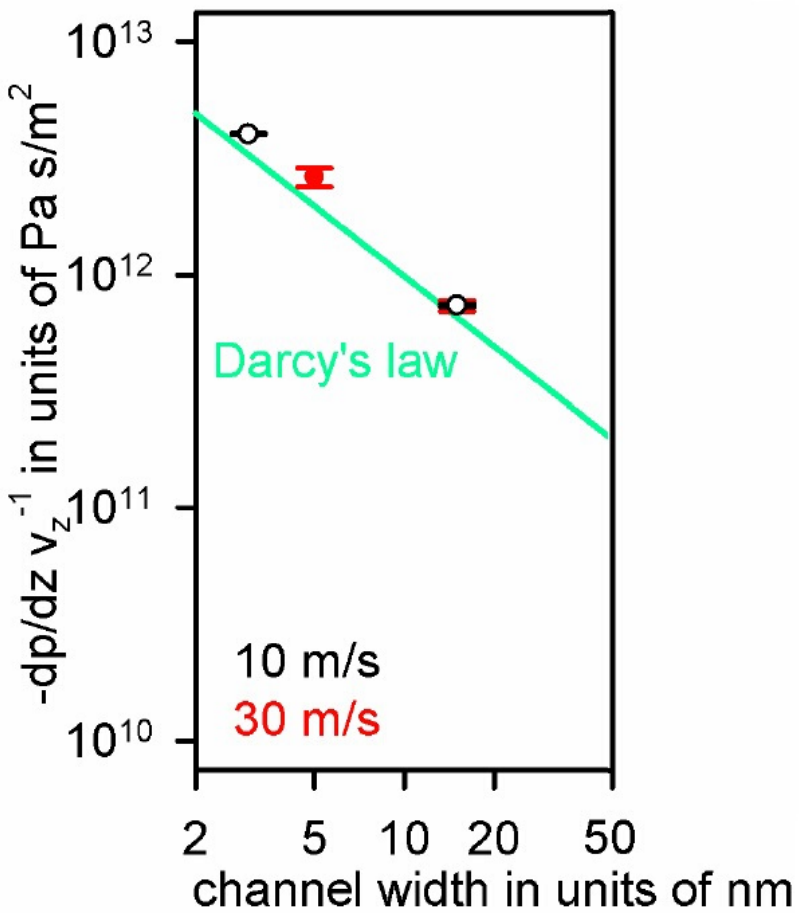

Nano- to microfluidics by scale-bridging MD

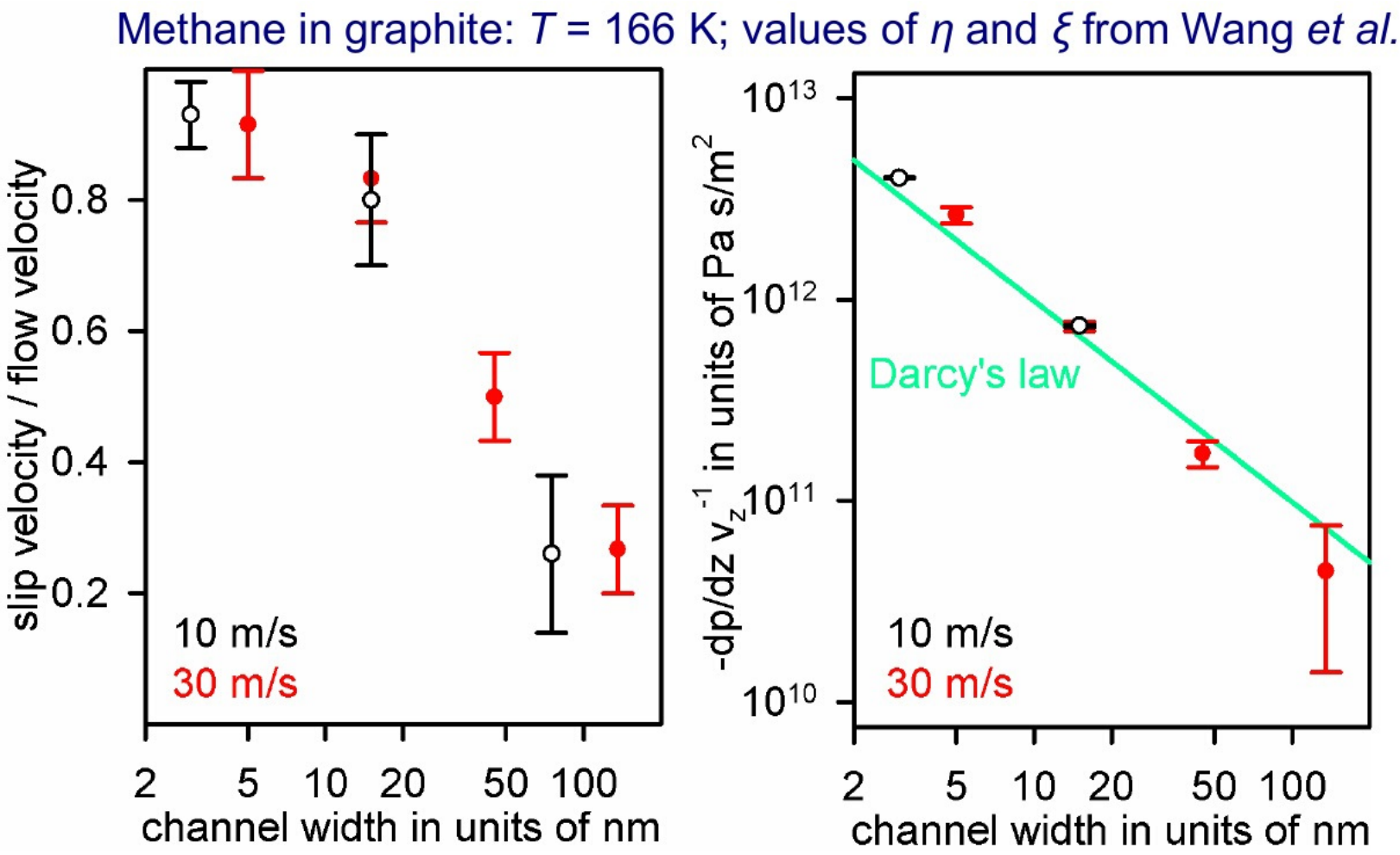

Scale bridging by mesoscopic approaches

Relaxation simulations based on a square-gradient **phase field model**:[1]

Allen-Cahn

$$\dot{\varphi} = -M \nabla_{\varphi} A$$

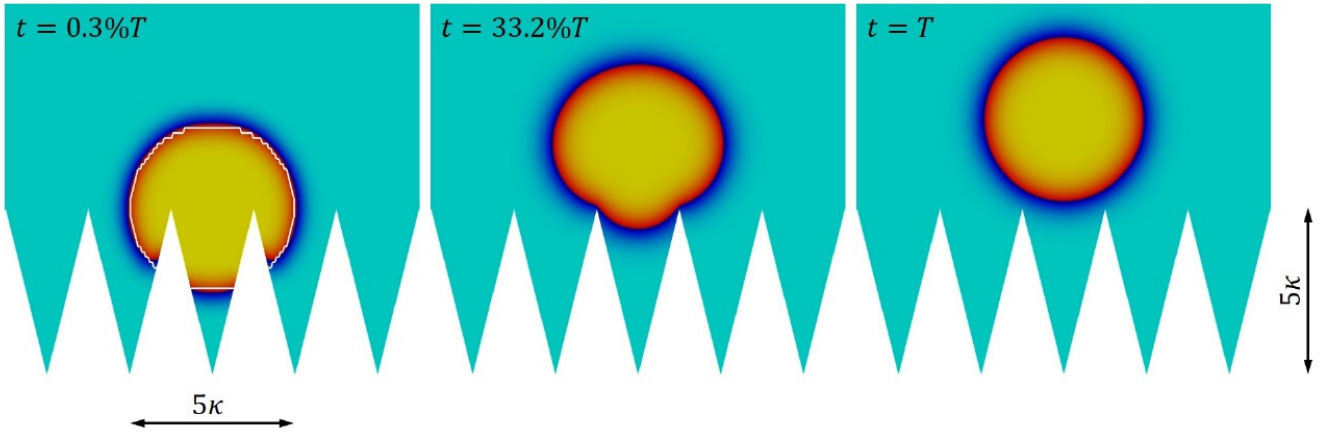

[1]F. Diewald, C. Kuhn, R. Blauwhoff, M. Heier, S. Becker, S. Werth, M. Horsch, H. Hasse, and R. Müller, *Proc. Appl. Math. Mech.* 16, 519, **2016**.

Scale bridging by mesoscopic approaches

Relaxation simulations based on a square-gradient **phase field model**:[1]

Allen-Cahn

$$\dot{\varphi} = -M \nabla_{\varphi} A$$

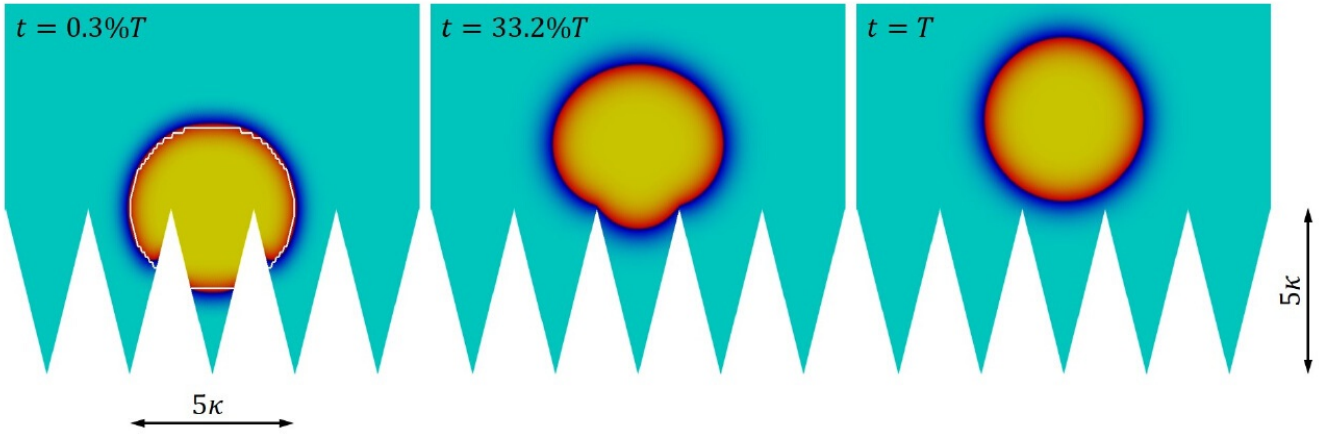

Future aims:

- Include inertia, external driving forces, non-equilibrium steady states
- Consider fluctuations, e.g. on the basis of fluctuating hydrodynamics

[1]F. Diewald, C. Kuhn, R. Blauwhoff, M. Heier, S. Becker, S. Werth, M. Horsch, H. Hasse, and R. Müller, *Proc. Appl. Math. Mech.* 16, 519, **2016**.

Conclusion

The increasing availability of HPC resources enables molecular simulation to capture the transition **from nano- to microfluidics** at an atomistic level. This is still expensive and does not make mesoscopic methods redundant. Instead, it helps **to validate theories and mesoscopic models**.

For phenomena involving fluid-solid contact, the **challenge to modelling and data science** consists in reducing the complexity of the fluid-solid interaction and surface morphology, retaining physically relevant features.

Example: The single-centre LJTS model captures the **influence of the fluid-solid dispersion energy** on the contact angle, the boundary slip length, and the Kapitza (thermal) resistance; all decrease as ζ increases.

However, **no lubrication** was found: Increased wetting of a model work piece by the LJTS fluid was found to increase the friction coefficient.